minerals

MDPI

Article

Mineralogical Tracers of Gold and Rare-Metal Mineralization in Eastern Kazakhstan

Boris A. D'yachkov [1,2,*], Ainel Y. Bissatova [1,3], Marina A. Mizernaya [1], Sergey V. Khromykh [4,5], Tatiana A. Oitseva [3], Oxana N. Kuzmina [1], Natalya A. Zimanovskaya [1] and Saltanat S. Aitbayeva [1]

1 Faculty of Earth and Environmental Sciences, D. Serikbayev East Kazakhstan Technical University, 19, Serikbayev Str., Ust-Kamenogorsk 070000, Kazakhstan; bisatova.ainelya@mail.ru (A.Y.B.); mizernaya58@bk.ru (M.A.M.); kik_kuzmins@mail.ru (O.N.K.); nata_zim@mail.ru (N.A.Z.); aitbayevass@mail.ru (S.S.A.)
2 Altai Geological and Environmental Institute LLP, 21, K. Libknekht Str., Ust-Kamenogorsk 070000, Kazakhstan
3 Geos LLP, 83, Protozanov str., Ust'-Kamenogorsk 070000, Kazakhstan; tanhic91@mail.ru
4 V.S. Sobolev Institute of Geology and Mineralogy, Siberian Branch of the Russian Academy of Sciences, 3, Koptyug Ave., 630090 Novosibirsk, Russia; serkhrom@igm.nsc.ru
5 Department of Geology and Geophysics, Novosibirsk State University, 1, Pirogova Str., 630090 Novosibirsk, Russia
* Correspondence: bdyachkov@mail.ru; Tel.: +7-(777)-152-18-42

Abstract: Replenishment of mineral resources, especially gold and rare metals, is critical for progress in the mining and metallurgical industry of Eastern Kazakhstan. To substantiate the scientific background for mineral exploration, we study microinclusions in minerals from gold and rare-metal fields, as well as trace-element patterns in ores and their hosts that may mark gold and rare-metal mineralization. The revealed compositions of gold-bearing sulfide ores and a number of typical minerals (magnetite, goethite, arsenopyrite, antimonite, gold and silver) and elements (Fe, Mn, Cu, Pb, Zn, As, and Sb) can serve as exploration guides. The analyzed samples contain rare micrometer lead (alamosite, kentrolite, melanotekite, cotunnite) and nickel (bunsenite, trevorite, gersdorffite) phases and accessory cassiterite, wolframite, scheelite, and microlite. The ores bear native gold (with Ag and Pt impurities) amenable to concentration by gravity and flotation methods. Multistage rare-metal pegmatite mineralization can be predicted from the presence of mineral assemblages including cleavelandite, muscovite, lepidolite, spodumene, pollucite, tantalite, microlite, etc. and such elements as Ta, Nb, Be, Li, Cs, and Sn. Pegmatite veins bear diverse Ta minerals (columbite, tantalite-columbite, manganotantalite, ixiolite, and microlite) that accumulated rare metals late during the evolution of the pegmatite magmatic system. The discovered mineralogical and geochemical criteria are useful for exploration purposes.

Keywords: gold deposit; rare metal deposit; mineral chemistry; mineral microinclusion; impurity; mineral potential; Eastern Kazakhstan

Citation: D'yachkov, B.A.; Bissatova, A.Y.; Mizernaya, M.A.; Khromykh, S.V.; Oitseva, T.A.; Kuzmina, O.N.; Zimanovskaya, N.A.; Aitbayeva, S.S. Mineralogical Tracers of Gold and Rare-Metal Mineralization in Eastern Kazakhstan. *Minerals* **2021**, *11*, 253. https://doi.org/10.3390/min11030253

Academic Editor: Joel E. Gagnon

Received: 20 December 2020
Accepted: 23 February 2021
Published: 28 February 2021

1. Introduction

The territory of Eastern Kazakhstan is an exceptional natural metallogenic laboratory which stores iron, copper, lead, gold, metals, rare earths, and other mineral resources that maintain a large mining and metallurgical industry [1]. Most of known mineral deposits were discovered by the classical geological prospecting in the second half of the 20th century. However, the pool of easily detectable deposits has been exhausted while the resources of the previous discoveries will be spent in a few decades of mining. The vertical structure of ore zones and their host formations have been poorly constrained so far, and the conventional exploration approaches become ever less workable in the metallogenic provinces of Eastern Kazakhstan. The progressive depletion of old mining areas calls for advances in exploration, especially for base, rare, and precious metals.

The detection of hidden, buried, and unconventional resources requires new prospecting and exploration technologies based on comprehensive knowledge of geology and

metallogeny. We have studied gold and rare metal mineralization in Eastern Kazakhstan for years while working for production enterprises [2–10]. Our results provided updates to the regional and local mineralization patterns, geological-genetic models, and exploration criteria for classification and appraisal of mineral resources [3]. However, constraining the age of gold and rare-metal deposits in the region and their linkage with igneous complexes requires further joint research efforts and a higher level of analytical work.

This paper focuses on search for mineralogical and geochemical tracers of gold and rare-metal mineralization in Eastern Kazakhstan using various advanced microscopy and analytical methods applied to samples of rocks, ores, minerals, and microinclusions from several potentially rich fields of Au sulfides and rare-metal pegmatites.

2. Geological Setting

The territory of Eastern Kazakhstan belongs to the Great Altai that encompasses areas near the borders of Kazakhstan, Russia, Mongolia, and China. The Great Altai structure formed in the course of Middle-Late Paleozoic collisional and accretionary interactions of Siberia with several Precambrian microcontinents and island arc terranes of the closing Paleoasian ocean which included the Ob-Zaisan oceanic basin [11–15]. Correspondingly, the territory accommodates numerous structures of active continental margins and paleooceanic settings: Southwestern Altai, including the Rundny Altai, Kalba-Narym, and West Kalba zones, along with the adjacent areas of Gorny Altai and Chinese Altai (Siberia); Chingiz-Tarbagatai and Zharma-Saur (Kazakhstan composite microcontinent); Char zone, a collage of ophiolite, siliceous pelagic sediment, and suprasubduction volcanic complexes (Figure 1).

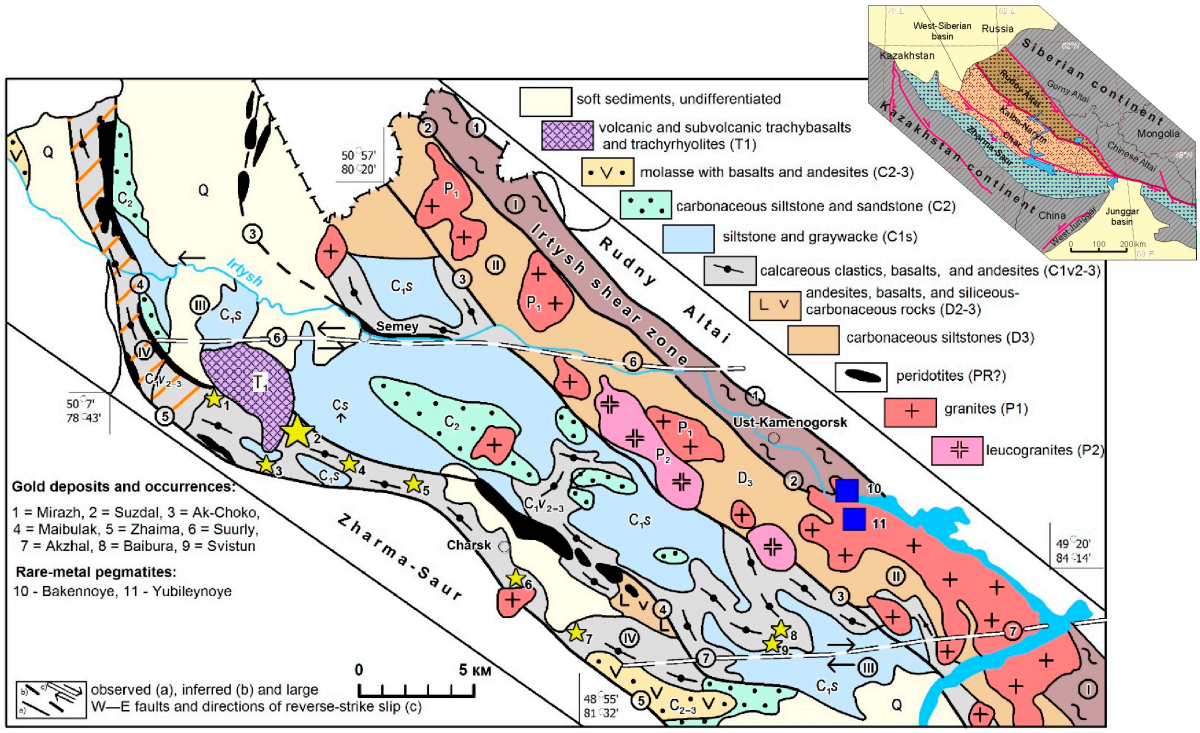

Figure 1. Gold and rare-metal mineralization in the Great Altai geological framework. Arabic numerals in circles stand for names of faults: 1 = Irtysh, 2 = Kalba-Narym, 3 = Terekta, 4 = Char, 5 = Baiguzin-Bulak, 6 = Semipalatinsk-Leninogorsk, 7 = Chingiz-Narym. Roman numerals in circles stand for names of shear zones: I = Irtysh, II = Kalba-Narym, III = West Kalba, IV = Char. Numbers 1 to 11 are gold (1–9) and pegmatite (10,11) deposits and occurrences (see legend).

The Great Altai metallogenic province comprises four parallel NW ore zones with their main mineralization types that formed in certain tectonic settings and conditions. They are the Rudny Altai copper-complex ore (Fe, Cu, Pb, Zn, Au, Ag, Pt etc), Kalba-Narym

rare-metal (Ta, Nb, Be, Li, Rb, Cs, Sn, W, TR), West Kalba gold (Au, Ag, Sb, etc.), and Zharma-Saur metal (Cr, Ni, Co, Cu, Hg, Au, Ag, W, Mo, TR) belts [5].

Gold mineralization in the Great Altai is known from the Rudny Altai, Char, and West Kalba zones. It is especially abundant in the Char and West Kalba zones but occurs mostly as a minor component in sulfide and complex ores in the Rudny Altai zone. The gold-bearing Fe, Mn, Cu, Zn, Pb, Au, Ag, etc. ores in the latter are associated with Devonian basalt-andesite-rhyolite volcanism ($D_{1–3}$) and controlled by large faults [2,3]. Many large and giant Cu, Pb, and Zn deposits of Rudny Altai (Orlovka, Artemiev, Ridder-Sokolny, Maleevsk, etc.) contain gold at average grades of 0.8–1.0 g/t Au, which makes a considerable share in the ore reserves of the region [6].

The gold deposits and occurrences in the Char and West Kalba zones (Figure 1) count more than 450, with the largest ones of Bakyrchik, Suzdal, and some others [2,3,5]. They show genetic links with gabbro-diorite-granodiorite-plagiogranite magmatism ($C_{2–3}$) and related fluid inputs channeled by a system of NW faults.

Gold-bearing sulfides (Figure 1) in the West Kalba belt exist as veins or disseminated mineralization in deformed island arc volcaniclastics of the Carboniferous ($C_1v_{2–3}$) Arkalyk Formation. The ore formation conditions were especially favorable in brecciated and fractured calcareous-carbonaceous siltstone and limestone with high percentages of sulfide phases. The known gold sites share similarity with typical gold deposits in metamorphosed carbonate rocks [16–18]. Gold in some fields (Suzdal, Zhaima, Mirazh, Baibura) occurs in brecciated, scarned, and quartzitized variegated limestones [8,19,20]. Primary ores include pyrite, goethite, arsenopyrite, gold, and accessory antimonite, pyrrhotite, chalcopyrite, galena, sphalerite, ilmenite, cinnabar, etc.

The Suzdal gold field is located at the boundary between the Char and West Kalba metallogenic zones. The host Arkalyk Fm. ($C_1v_{2–3}ar$) is composed of calcareous- carbonaceous-clayey silt, fine sand, massive crinoidal limestone, and moderate amounts of porphyritic andesite and tuffite (Figure 2). The intrusive rocks of the area are diorite porphyry (dikes) and granodiorites of the Kunush complex (C_3). The mineralization is mainly controlled by the 700–1300 m wide Suzdal fault zone of quasi-parallel NE faults dipping in the SE direction at 40–60°. Four 10–25 m thick ore zones in the field have been explored to a depth of 500 m. Nest-like, vein, or disseminated gold-bearing sulfide mineralization occurs in heavily deformed sediments. The orebodies are mainly localized in the middle of ore zones (Figure 3).

Some other occurrences and sites in the West Kalba and Char zones (Baibura, Zhaima, etc.) are potentially rich in gold-bearing sulfide ores as well (Figure 1).

The rare-metal deposits within the Great Altai mainly occur within the Kalba-Narym belt and are related with Permian postcollisional granitic magmatism [7,10,21–23]. Rare-metal pegmatites in the Central Kalba ore district (Figure 4) host the largest pegmatitic (Bakennoye, Yubileinoye, Belaya Gora, Upper Baimurza, etc.) and potentially Sn-Ta-Li-bearing apogranitic albitite-greisen (Karasu, Novo-Akhmirovo, Tortkalmak etc.) deposits and smaller greisen-quartz vein and hydrothermal deposits and occurrences (Sn, W), as well as tantalite, cassiterite, wolframite, and scheelite placers. The pegmatite deposits are of three main types: blocky microcline (i), rare-metal (ii), or crystal-bearing chamber (iii) pegmatites [9,10,23].

The mineralogical and geochemical exploration criteria were revealed in several reference rare-metal pegmatite deposits from the Kalba-Narym zone (Asubulak, Bakennoye, etc.).

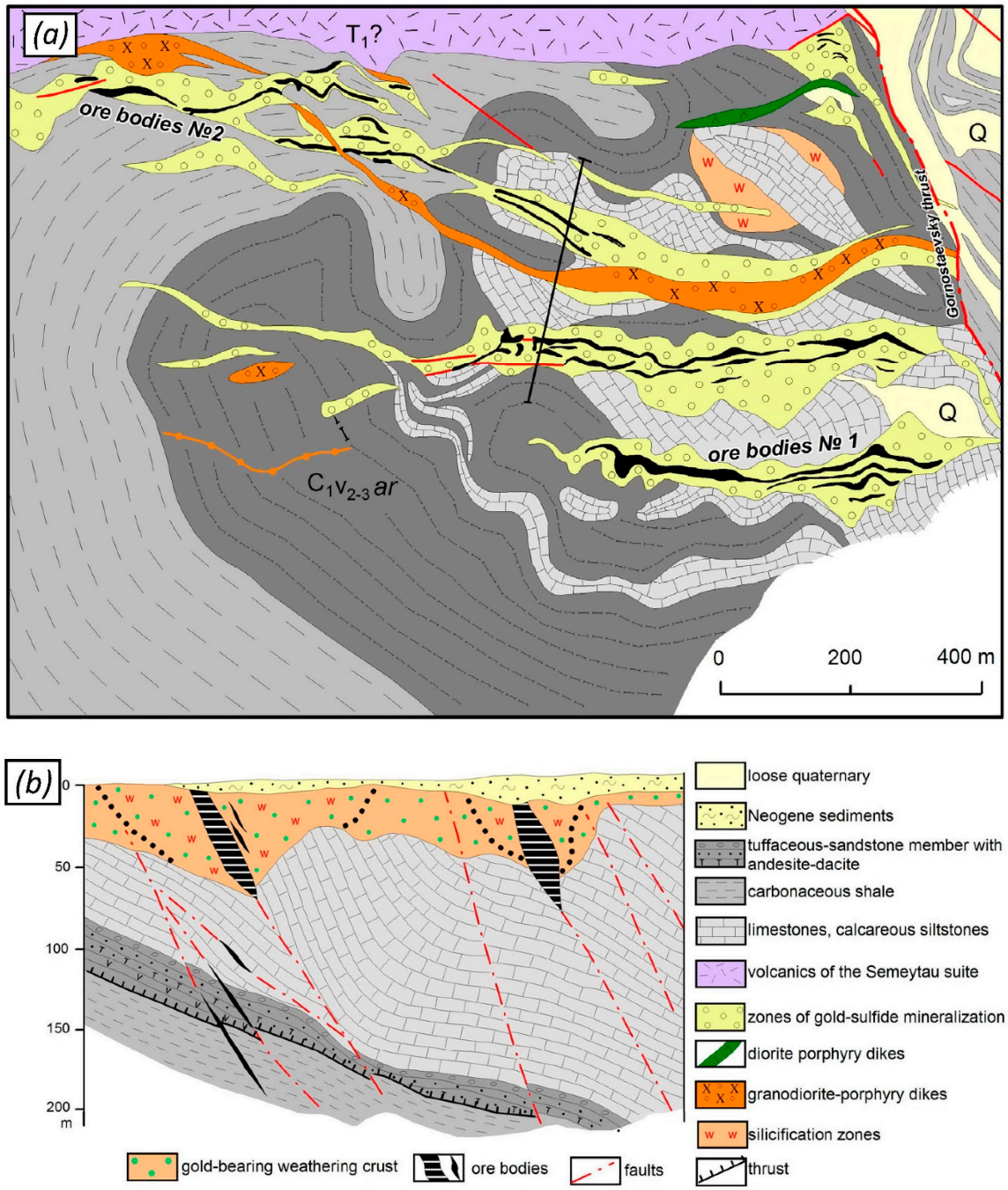

Figure 2. Local geology of the Suzdal gold field (map view (**a**) and cross section (**b**)), after geological reports by I.V. Begaeva and V.A. Denisenko.

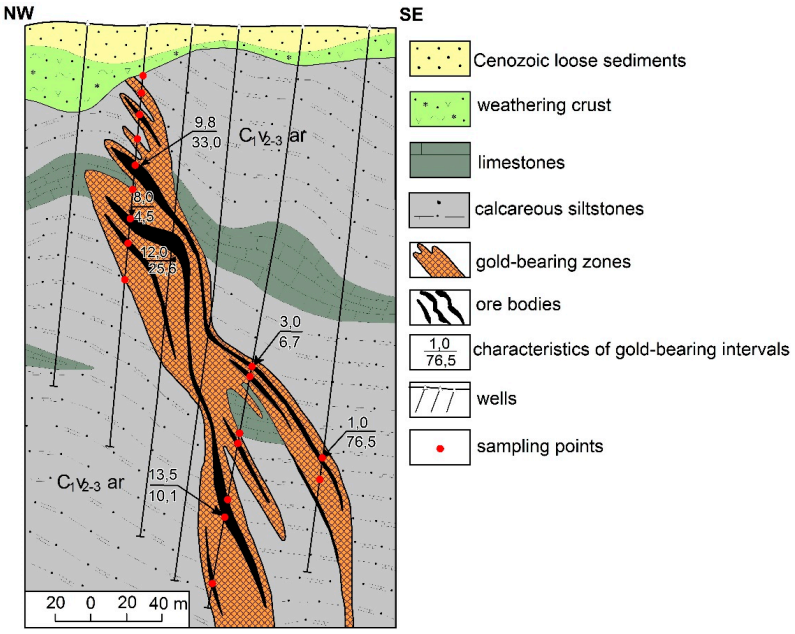

Figure 3. An ore zone in Suzdal gold deposit, after geological reports by I.V. Begaeva. Numerals show thickness of gold-bearing intervals (above bar) and average gold grades in g/t Au (below bar). Soft sediments Weather ed rocks Gold-bearing intervals Boreholes.

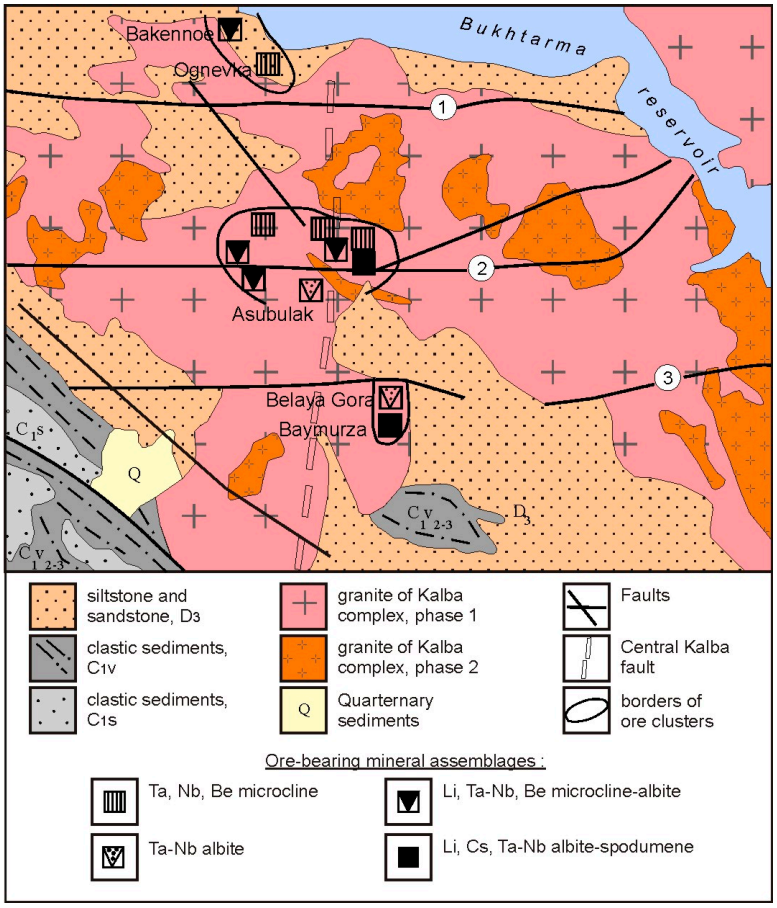

Figure 4. Geological map of the Central Kalba ore district and location of rare-metal pegmatite deposits, after [10]. Numerals 1 to 3 are Gremyachy-Kina (1), Asubulak (2), and Pervomaysk-Belogorsk (3) faults.

3. Materials and Methods

The work began with field examination and sampling at typical gold and rare-metal deposits in Eastern Kazakhstan. We collected mainly 0.5–1.0 kg samples of sedimentary, volcanic, and intrusive rocks and ores, including gold-bearing jasperoids, gold-quartz-carbonate-sulfide metasomatics, quartz veins, etc. (5–6 samples of each rock and ore type on average). The location of samples is shown on the Figure 3. Native gold particles of 0.05 to 0.375 mm sizes were extracted from six 12–15 kg samples of ironstones from weathered zones. The samples of hornfels and fresh or altered granites, as well as pegmatitic minerals of simple oligoclase-microcline to complex albite-spodumene assemblages represented the rare-metal pegmatite deposits.

The laboratory procedures included separation of monomineral fractions (pyrite, muscovite, lepidolite, spodumene, tourmaline, quartz, cassiterite, etc.) and various analyses. The compositions of rocks and minerals were determined, respectively, by mass spectrometry with inductively coupled plasma (ICP-MS) on an Agilent 7500cx (Agilent Technologies, Santa Clara, CA, USA) spectrometer and by electron probe microanalysis (EMPA) on a Cameca MS-46 (Cameca, Gennevilliers, France) analyzer that allowed detection and precise measurements of seventy three elements (Au, Ag, Pt, Cd, In, Ir, Y, Cd, TR, U, etc.). The analytical procedures were performed at VERITAS Laboratory of the D. Serikbaev East Kazakhstan Technical University (Ust'-Kamenogorsk) and at the Analytical Center of the V. Sobolev Institute of Geology and Mineralogy (Novosibirsk). Scanning electron microscopy and energy dispersive spectrometry (SEM-EDS) was applied to study micrometer inclusions of opaque and related minerals and to analyze impurity elements (Au, Ag, Pt, In et al.). The instruments were a Jeol-100C microscope with a Kevex-Ray detector and a Jeol ISM-6390 LV microscope with an Oxford INCA Energy system (JEOL, Tokyo, Japan). The major-element chemistry was analyzed by the X-ray fluorescence (XRF) method. The Au and Ag contents in ores were determined by atomic-absorption spectrometry (AAS).

4. Results

4.1. Tracers of Gold Mineralization

The primary ores of the Suzdal gold deposit consist of pyrite, goethite, arsenopyrite, and gold as main minerals and accessory antimonite, pyrrhotite, chalcopyrite, galena, sphalerite, ilmenite, cinnabar, etc. The rock matrix minerals are quartz, siderite, calcite, and K-Al silicates. Gold is either disseminated in pyrite and arsenopyrite or appears as submicrometer to 100–150 μm particles in the primary sulfide ores. The gold mineralization is very unevenly distributed, with average grades reaching 9 g/t Au in economic ores. It is traced by Fe, As, Sb, Cu, Pb, and Zn sulfide minerals in ores and their limestone hosts.

The sulfide ores of the Suzdal gold deposit occur within hydrothermally altered calcareous-carbonaceous sediments cut by faults and dikes. The deposit shares some features: (1) limestone and calcareous sedimentary hosts; (2) spatial proximity to small intrusions and dikes; (3) alteration patterns, including iron-siliceous metasomatism, jasperoid quartzitization, argillization, etc.; (4) ore mineralogy consisting of pyrite, arsenopyrite, gold, barite, calcite, cinnabar, etc.); (5) high gold contents.

The ores in the Baibura deposit are especially abundant in brecciated ironstones from the weathered zone, with numerous nests or disseminated particles of oxidized sulfide minerals and visible gold (Figure 5).

The mineralization is traced by Fe, Mn, Al, As, Sb, Cu, Pb, Zn, Ag, Au, and other elements that were supplied into the system. Typical minerals in gold-bearing sulfide ores (Figure 6) are goethite, magnetite, arsenopyrite, antimonite, galena, gold, silver, etc.

We revealed a number of previously undetected phases (magnetite, brownite, PGE xenotime and rare-metal bearing cassiterite, scheelite, microlite), as well as rare phases of Pb (alamosite, kentrolite, melanotekite, cotunnite) and Ni (bunsenite, trevorite (?), gersdorffite, etc.), which shed more light on ore compositions.

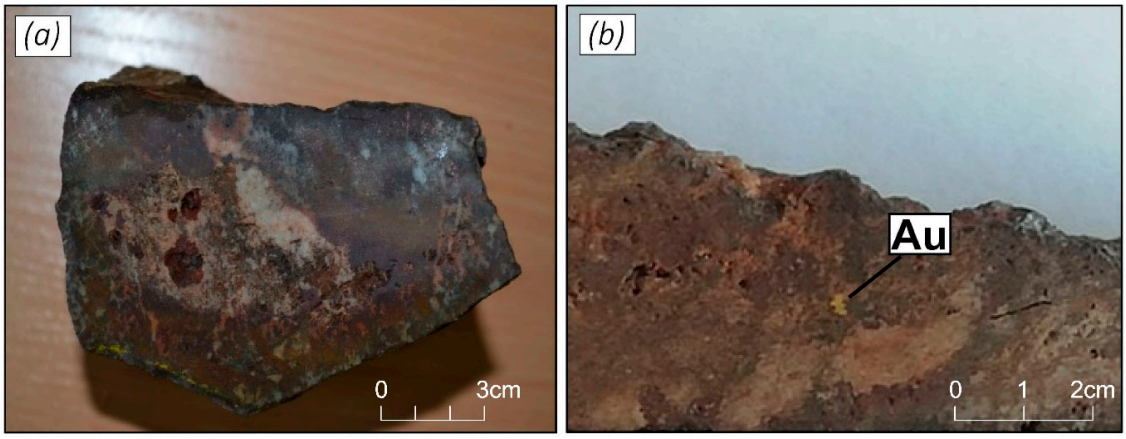

Figure 5. Gold-bearing ironstone, Baibura site: brecciated ironstone with nests of sulfides and metasomatic quartz (**a**); free gold, 3 mm particles (**b**).

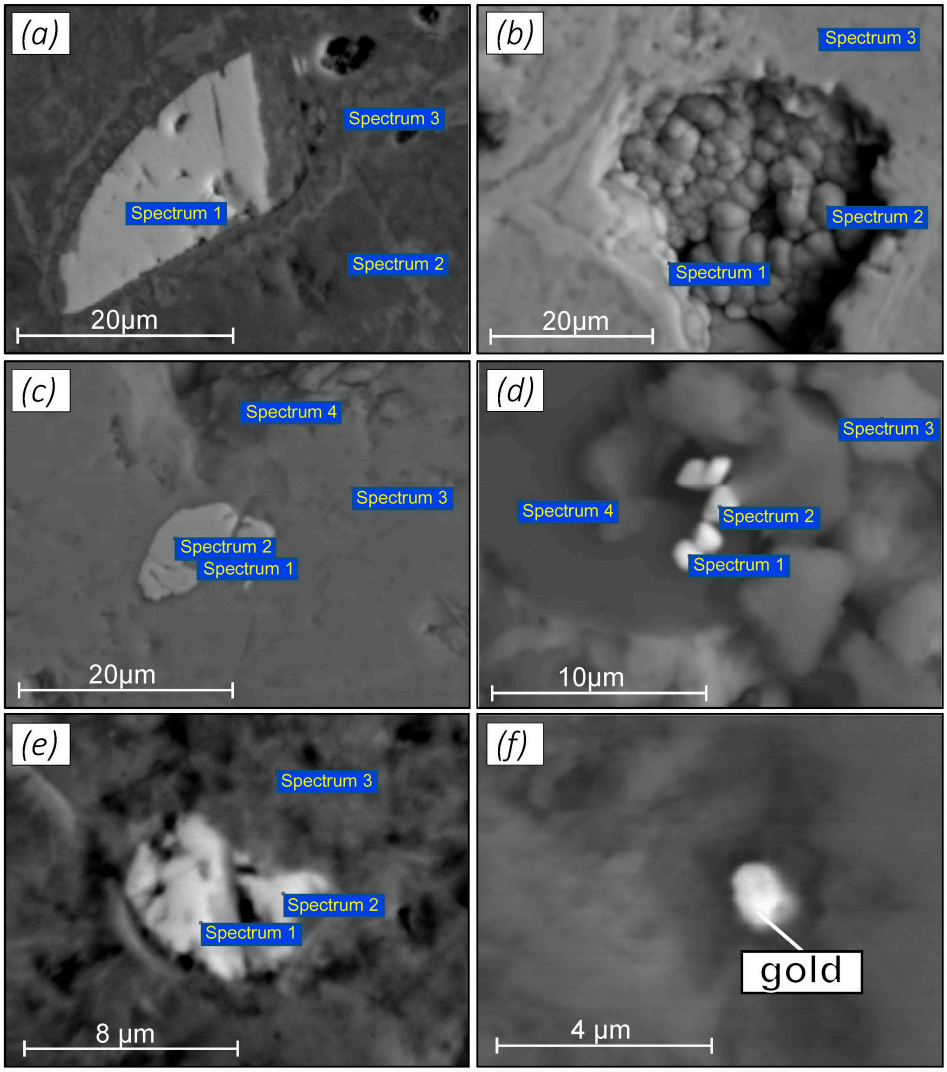

Figure 6. Microinclusions in sulfides and related minerals in limestone and metasomatitc rocks, Rodnikovaya zone: euhedral arsenopyrite (**a**); iron hydroxide oolites (**b**); euhedral arsenopyrite in jasperoid (**c**); galena in quartz (**d**); pyrite (**e**); gold in metasomatic quartz (**f**).

Native gold was separated from jasperoids (with participation of S. Petrov), identified with reference to the morphological classifications of L. Nikolaeva and S. Yablokova et al. (Central Research Institute for Geological Prospecting, Moscow), and documented using a Motic 352 digital microscope camera (Motic, Xiamen, China), a LOMO MBS-10 binocular stereomicroscope (LOMO, Saint Petersburg, Russia), and an Olimpus M780 camera (Olympus Corporation, Tokyo, Japan). The extracted sixty one gold particles varied in size from 0.027 to 0.267 mm (mean 0.085 mm). Many were of dust 0.05–0.1 mm (45.9%) and very fine 0.1–0.25 mm (42.6%) size fractions, while the fine dust 0.01–0.05 and fine 0.25–1.0 mm fractions were limited (Figure 7).

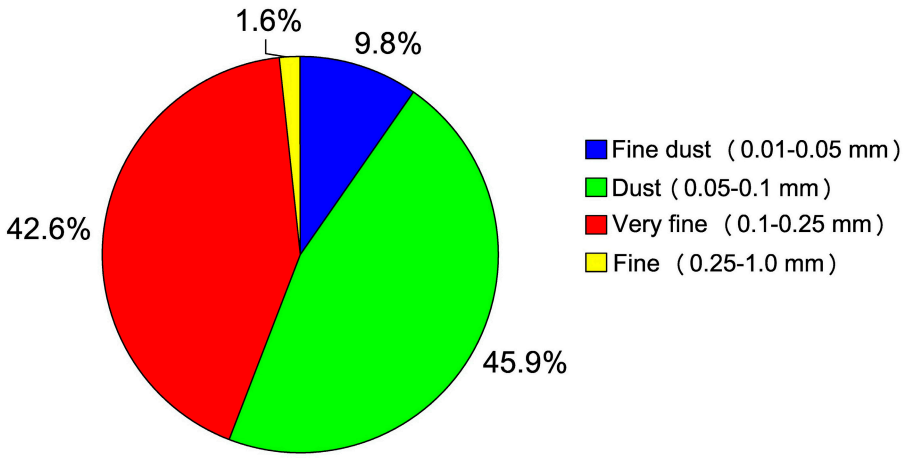

Figure 7. Size distribution of gold particles. Sample P-20 (N = 61), Baibura deposit.

According to EMPA, gold is of 932–935‰ fineness, with 0.333–0.487 wt.% Hg impurity. Some particles (26.2%) retain faceted contours and many (90.2%) bear matrix imprints. The particles have platelet (68.9%) or flaky (24.6%) shapes; most of them have >0.5 flatness and can be separated by flotation (75.4% of all particles), and others are amenable to gravity concentration.

According to Cameca MS-46 microprobe data (Figure 8) the gold particles have 150 to 400 μm sizes and flaky, platelet, or elongate shapes; some make nests or are intergrown with quartz, hydrogoethite, or rock.

Gold and silver also exist in μm to tens of μm microinclusions detected under an ISM-6390 microscope (JEOL, Tokyo, Japan) at defect sites on the surface of jasperoids (Figure 9a,b). The inclusions contain Ag (3.32 wt.%), W (2.15 wt.%), and Rb (1.75 wt.%) impurities. Some samples of semi-oxidized quartz-carbonate-sulfide metasomatite bear coarser matrix-affected gold grains, like the dense particle in Figure 9d consisting of 88.49 wt.% Au, with 9.59 wt.% Ag and 1.92 wt.% Pt (total 100%).

Of special interest are rare-metal phases found in Au sulfide zones, which were previously considered alien to gold mineralization. They are microinclusions of cassiterite (39.28 wt.% Sn, 2.28 wt.% Ta), hübnerite (45.61 wt.% W, 38.26 wt.% Mn) and scheelite (45.61 wt.% W), with high contents of trace elements (10.04 to 46.80 ppm Sn, 14.66 ppm Nb, and 4.94 ppm Ta) determined by mass spectrometry.

Gold-bearing sulfide ores in some fields (Zhaima, Baibura) coexist with hydrothermal manganese mineralization (brownite, rhodochrosite, hausmannite, pyrolusite, etc.). Massive brownite (Mn_2O_3) is a typomorphic phase, which often bears nests or impregnation of rhodochrosite and miaroles of quartz-topaz-feldspar (Figure 10). It contains 53.06 wt.% MnO, high or relatively high contents of Cu (10,370 ppm), Zn (10,240 ppm) and Pb (2071 ppm), W (513.5 ppm), Sb (393.6 ppm), Ag (156 ppm), and 0.26 ppm Au (ICP-MS data). Trace elements are Ta (25 ppm), Be (43 ppm), Li (282 ppm), Rb (58.2 ppm), and Sn (168.3 ppm); the contents of Eu (10.95 ppm) and some other rare earths (25.68 ppm Gd, 6.01 Tb, 18.19 ppm Dy, 9.48 ppm Er, and 6.89 ppm Yb) are above average values for upper

continental crust (according to [24]); anomalously high Sr contents (1382–1929 ppm) may record a deep crust-mantle source of primary fluids.

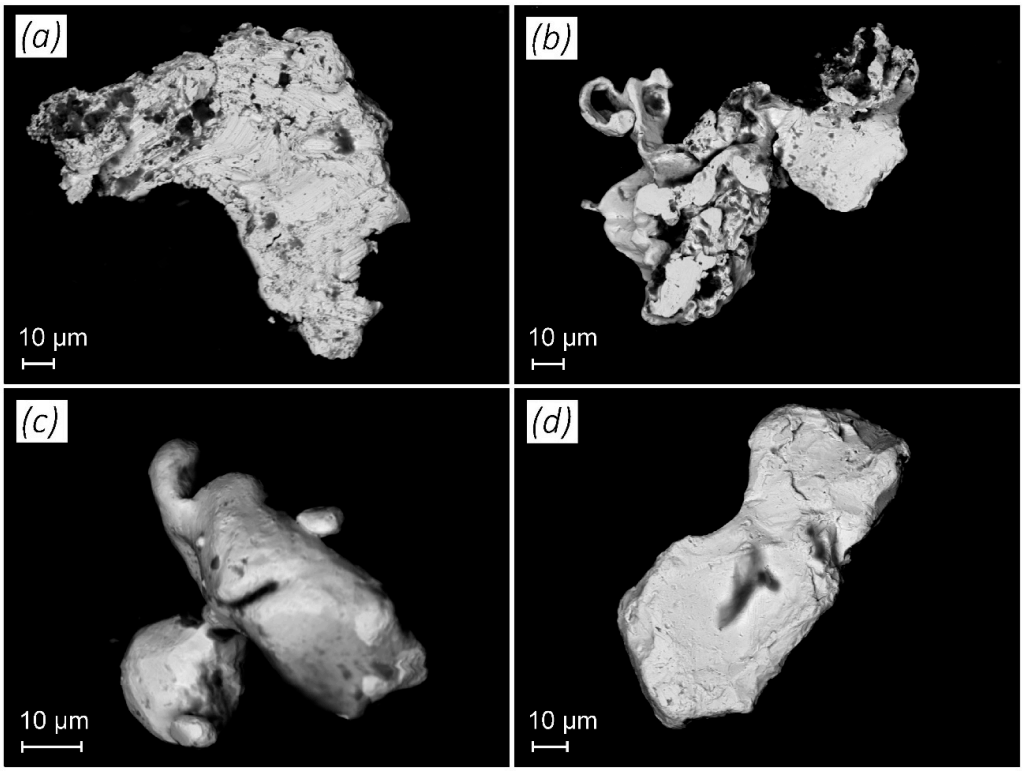

Figure 8. Native gold particles: platelet gold attached to rock (**a**), intricately shaped particle (**b**), flaky gold (**c**), massive platy gold (**d**).

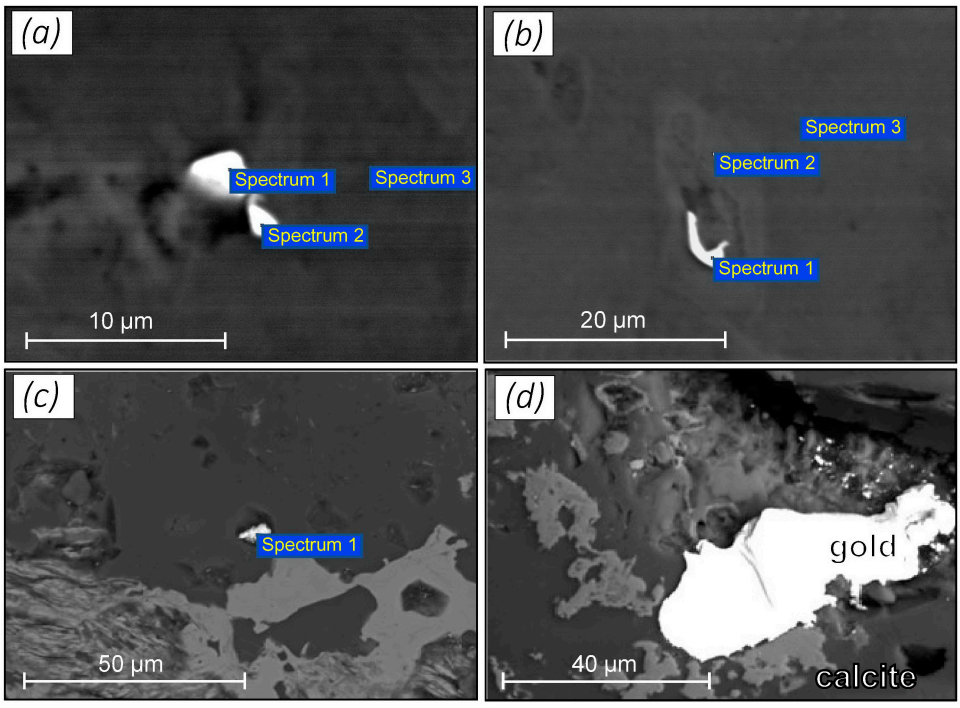

Figure 9. Gold and silver microinclusions in weathered ironstone: flaky (**a**) and crescent-shaped (**b**) particles on jasperoid surface; submicron silver inclusions (**c**), relatively large massive particles in quartz-carbonate-sulfide metasomatite (**d**).

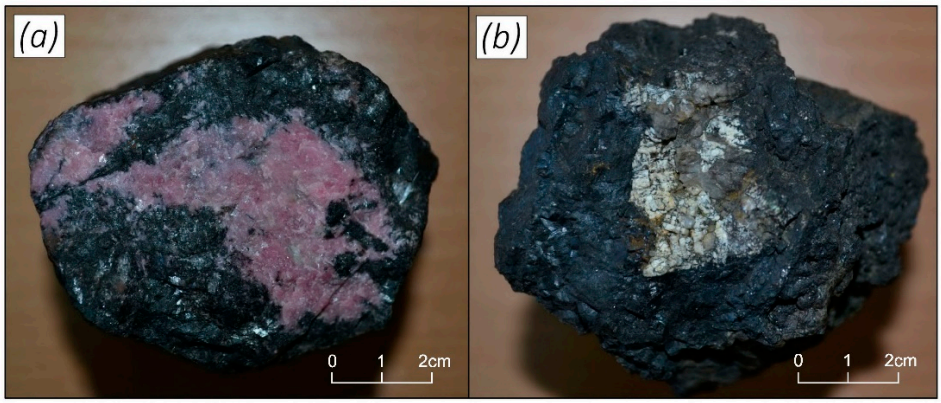

Figure 10. Manganese ore, Baibura site: massive brownite with pink rhodochrosite (**a**) and quartz-topaz-feldspar miaroles (**b**).

Brownite encloses many minerals (apatite, arsenopyrite, antimonite, galena, hübnerite, uraninite, etc.), as well as rare Pb phases never found before (Figure 11): alamosite ($PbSiO_3$), melanotekite ($Pb_3Fe_4Si_3O_{15}$), kentrolite ($Pb_3Mn_4Si_3O_{18}$), cotunnite ($PbCl_2$), and gersdorffite (NiAsS).

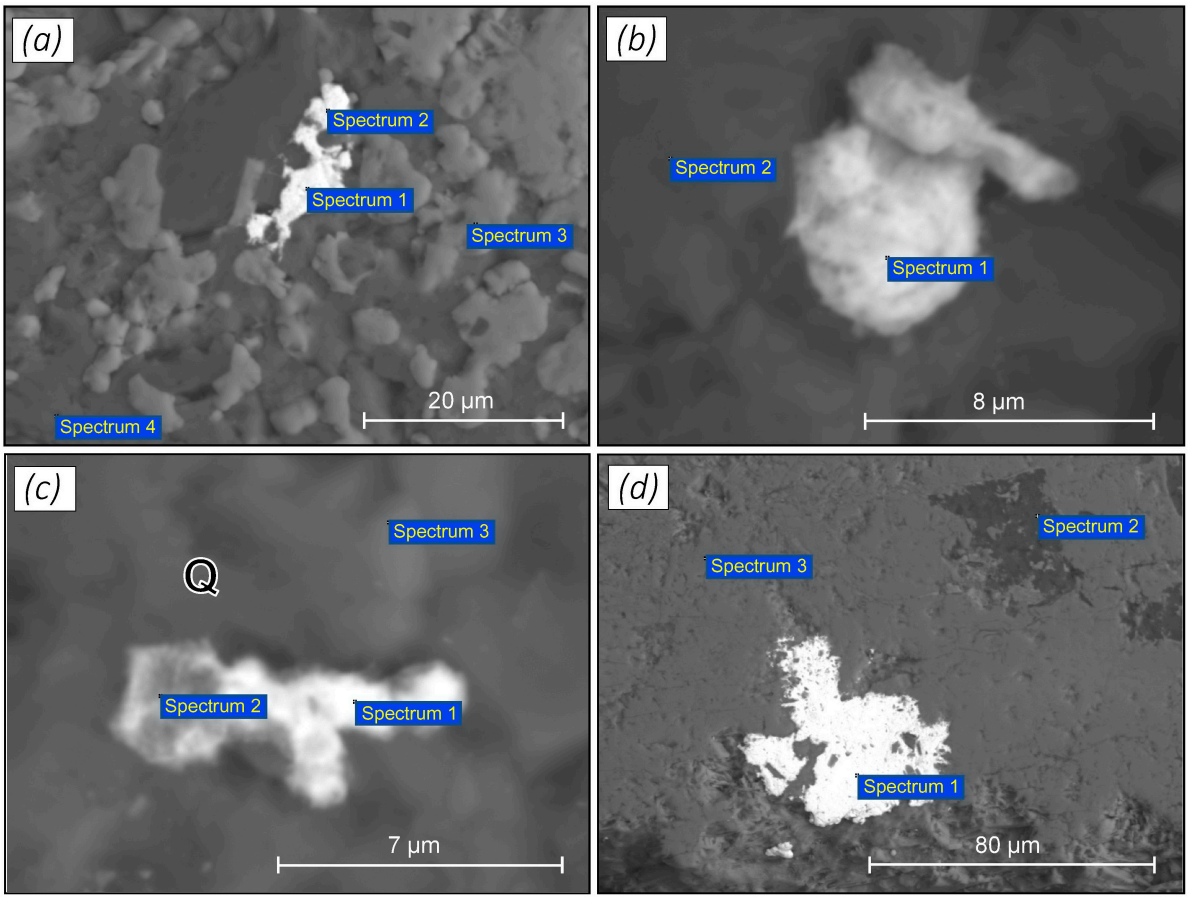

Figure 11. Microinclusions of rare phases in manganese ores: round (**a**) and irregularly shaped (**b**) alamosite, disseminated melanotekite (**c**), and intricately shaped disseminated kentrolite (**d**).

Alamosite is a rare Pb phase known from weathered zones of lead deposits [25]. In Eastern Kazakhstan, we discovered this mineral at the Baibura deposit in the West Kalba zone, where gold and manganese fields are spatially proximal. Alamosite and other Pb

minerals were found in manganese ores containing elevated concentrations of Pb, Cu, Zn and other metals. SEM analysis of pure alamosite varieties showed a relatively uniform Si:O:Pb proportion of 1:2.2:5.4, with a total of 100%. Micrometer alamosite grains in thin quartz-manganese veins have intricate shapes and rough surfaces. High concentrations of trace elements were determined in Zhezdy, Zhomart, and other hydrothermal Mn deposits of Central Kazakhstan [26]. Therefore, the presence of manganese ores coexisting with gold mineralization can be considered as a good exploration guide.

Magnetite (up to 3–5 mm) in mineralization zones traceable by magnetic anomalies reaching 2250 nT also has diagnostic value. Polished sections exhibit ilmenite replacing magnetite and inclusions of antimony (53.19 wt.% Sb, 20.62 wt.% S), galena (49.60 wt.% Pb), cotunnite ($PbCl_2$) and native silver with copper impurity (47.51 wt.% Ag, 1.99 wt.% Cu).

Auriferous sulfide oxide zones sometimes bear nickel phases of bunsenite (87.13 wt.% Ni, 11.50 wt.% O, 1.37 wt.% Si) and a P-bearing mineral (62.34 wt.% Ni, 15.12 wt.% O, 6.51 wt.% P, 5.35 wt.% Fe) found as flaky particles or as rims around magnetite (Figure 12). This may be a variety of trevorite ($NiFe_2O_4$) or nickelphosphide $(Ni, Fe)_3P$ [27,28].

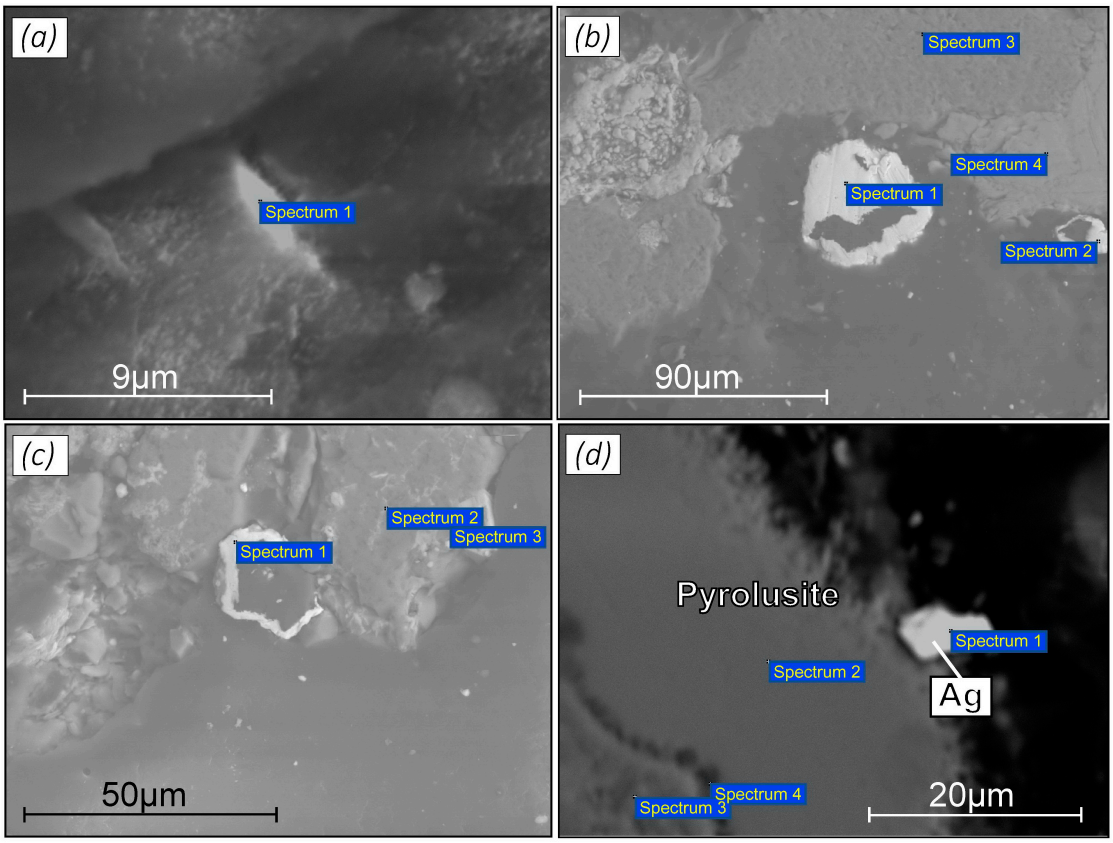

Figure 12. Microinclusions of Ni-bearing minerals and native silver in weathered Au sulfide ores: bunsenite (**a**); trevorite (**b**); loop-shaped trevorite? (**c**); silver (51.12 wt.% Ag, 2.65 wt.% Cu) at pyrolusite/quartz boundary (**d**).

Thus, Suzdal-type apocarbonate gold ores have complex compositions, with phases of lithophile, chalcophile, siderophile and other elements. The presence of HREEs (Dy, Er, Yb), PGE (Ir, Pt), Fe, Ni, Co, Cr, Au, W, Ta, and U, as well as quite high contents of Sr, record a crust-mantle source of primary ores. The ores bear free gold of different particle shapes and sizes (from fine dust to fine fractions), which is amenable to gravity and flotation concentration. Typical opaque minerals include magnetite, hematite, goethite, pyrite, arsenopyrite, Mn phases, galena, chalcopyrite, and sphalerite coexisting with rare-metal and REE phases.

Such trace elements as Fe, Mn, As, Sb, Cu, Pb, Zn, Ag, Sn, W, and Ba are main tracers of gold mineralization. The revealed minerals and elements can be used in exploration as guides to new gold fields and occurrences.

4.2. Tracers of Rare-Metal Mineralization

Pegmatite ore formation was modeled as pulse-like rhythmic inputs of metal-laden gas-liquid fluids (H_2O, F, B, Cl, Ta, Sn, Be, etc.) from crustal magma sources through faulted crust, synchronously with granitic magmatism [10,23]. The Kalba-Narym rare-metal pegmatites are spatially and genetically linked with medium-coarse porphyritic phase I Bi granites (P_1) of the Kalba complex [10].

The pegmatites evolved at variable pressure, temperature, pH, and alkalinity conditions while mineral assemblages underwent metasomatic alteration with formation of secondary microcline, albite, greisen, spodumene, etc. and changed from simple barren graphic and oligoclase-microcline pegmatite to Li-bearing microcline-albite, quartz-albite-muscovite (greisen), quartz-albite-spodumene varieties with progressively increasing concentrations of Ta, Nb, Be, Li, Cs, Sn, and TR. These trends are consistent with the general evolution of pegmatites and rare-metal (Ta, Be, Li, Cs, Sn, TR, etc.) mineralization [29–32]. Mineralization is especially high in pegmatite veins bearing signatures of multiple metasomatic events that produced unique mineral phases, such as cleavelandite, lepidolite, spodumene, ambligonite, pollucite, color tourmaline, tantalite-columbite, etc.). The ores consist of tantalite-columbite, beryl, cassiterite, spodumene, and pollucite; the vein phases are quartz, microcline, albite, muscovite, shorl, etc.

Scanning electron microscopy has provided new data on mineralogy and chemistry of ores and distribution of impurities in Ta, Li, and other phases in pegmatites. It also revealed rare minerals, which remained undetectable by semi-quantitative laboratory methods, as well as typical minerals and trace elements that may be indicators of rare-metal mineralization.

Tantalite (Fe, $MnTa_2O_6$), a main opaque mineral, occurs as brownish to black short-prismatic or tabular crystals or as impregnation in albitized pegmatite (Figure 13).

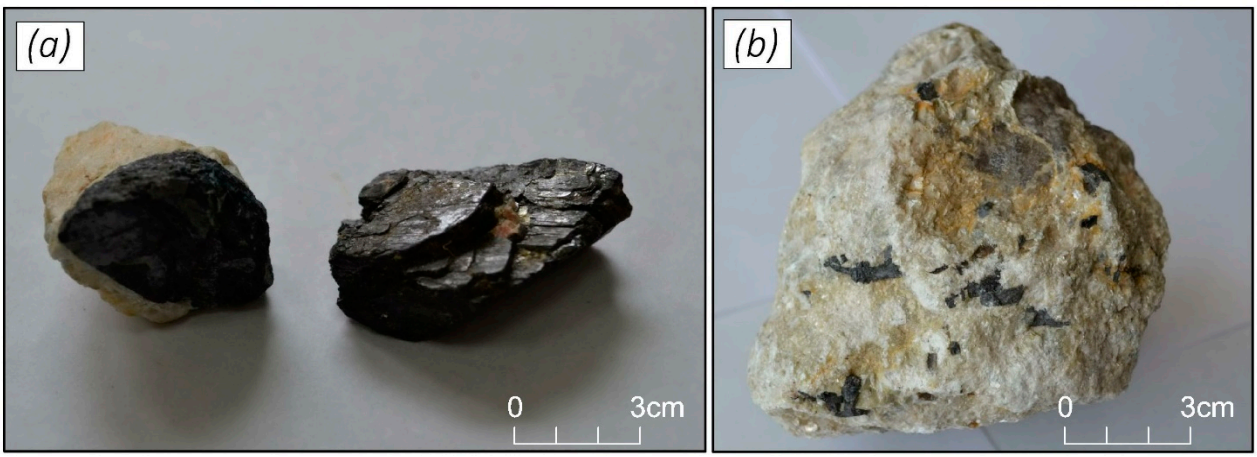

Figure 13. Ta-bearing minerals, Yubileinoye deposit: tantalite-columbite crystals (**a**) and inclusions in albitized pegmatite (**b**).

Some crystals have dipyramidal s {121} and e {112}, prismatic h {001}, and pinacoidal h {010} faces. The composition trends of Ta-bearing minerals (Fe, Mn, Ta, Nb) and increasing concentrations of impurities (Li, Rb, Cs, Sn, W, Zr, U, TR, etc.) record a mineralization history of at least two stages: early Fe-rich tantalite-columbite and tapiolite-Fe $(Ta, Nb)_2O_6$ and late tantalite-columbite, manganotantalite, ixiolite, and microlite (Figure 14).

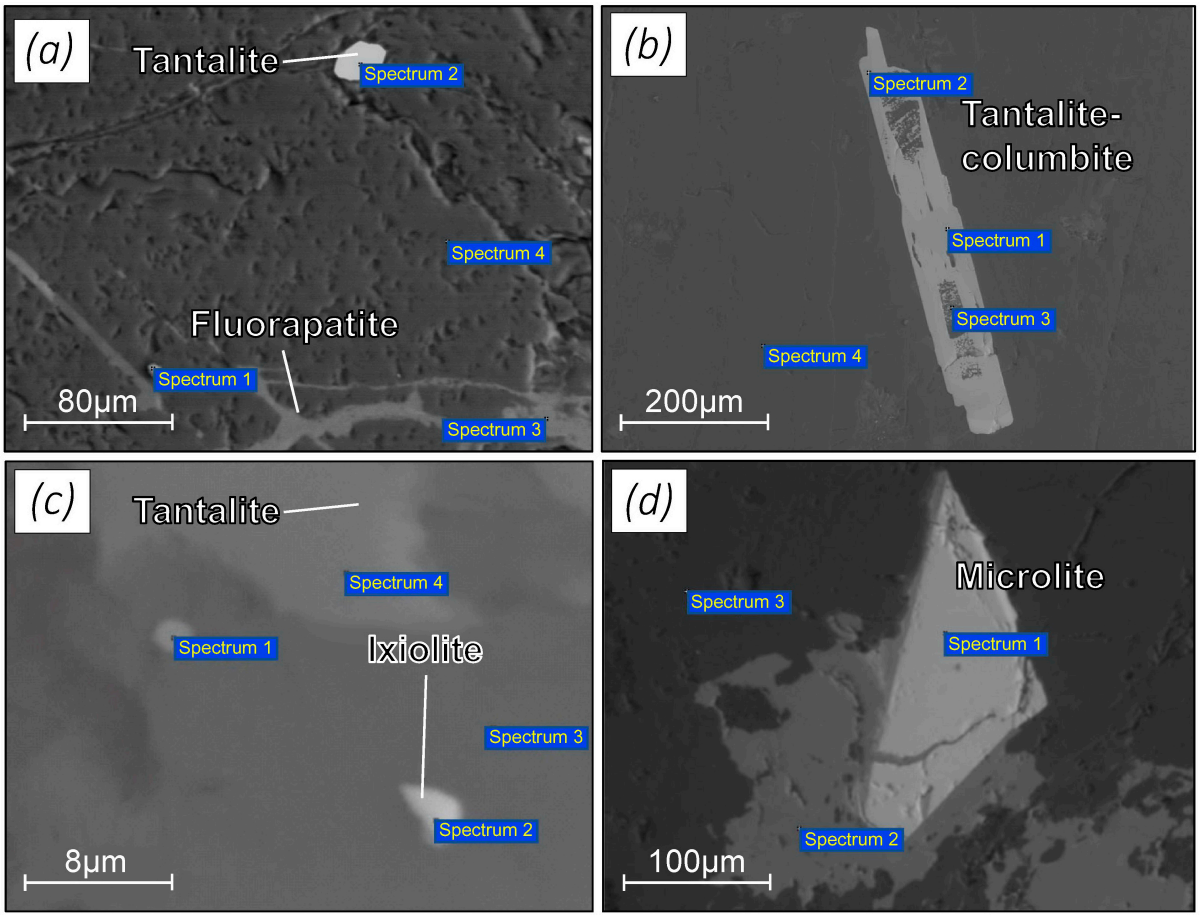

Figure 14. Microinclusions of Ta-bearing minerals: tantalite flakes and fluorapatite streaks (**a**); long prismatic columbite (**b**); ixiolite (**c**); microlite (**d**).

Manganotantalite, a main phase of commercial ores, is a manganese variety of tantalite that contains 67.8 wt.% Ta_2O_5, 16.9 wt.% Nb_2O_5, 14.7 wt.% MnO, 0.73 wt.% FeO, and 0.9 wt.% SnO_2. High Mn contents are confirmed by SEM: 16.33 wt.% MnO and 0.71 wt.% FeO according to BSE spectra; Mn/Fe > 8.4 from mass spectrometry. SEM analysis shows 28.27 wt.% Ta, 27.44 wt.% Nb, 10.13 wt.% Mn, and 33.60 wt.% O, at low to absent Fe (Figure 15).

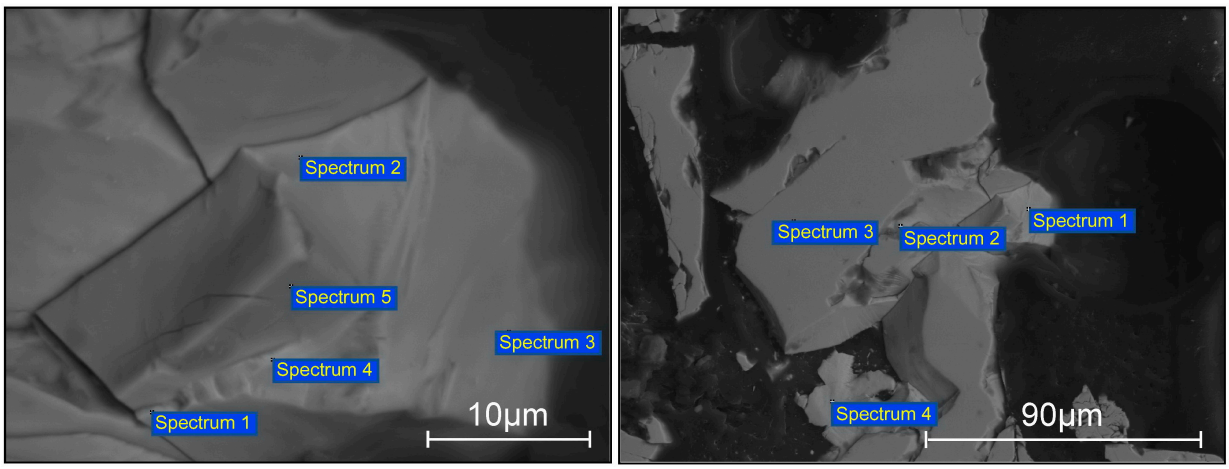

Figure 15. SEM image of massive manganotantalites.

Tantalite contains ≤30 ppm ΣREE, with light REE enrichment over heavy REE (LREE/HREE = 1.9 to 6.4); other elements reach 65.34 ppm Cu, 106.3 ppm Zn, 28.5 ppm Pb, 3932 ppm Ti, 116.1 Ba, 181 ppm Sc, as well as Sn, W, and alkali impurities (Table 1). Late-generation tantalite is rich in Zr (2800–8734 ppm), Hf (490–622 ppm), and U (up to 1243 ppm) and extremely rich in In (up to 266 ppm) due to cassiterite impregnation. We discovered noble metals in tantalite: unevenly distributed Au, Ag, Pt, Ir, Cd, and Sb, with the highest concentrations of >53 ppm Au, 15 ppm Ag, 41 ppm Pt, and 11 ppm Ir. SEM (Figure 16) revealed nanometer inclusions of Ta, W, Au, Hf, and U in microlite (56.6 wt.% Ta) and 9.37 wt.% U, 8.09 wt.% Pb, and 4.62 wt.% W contents.

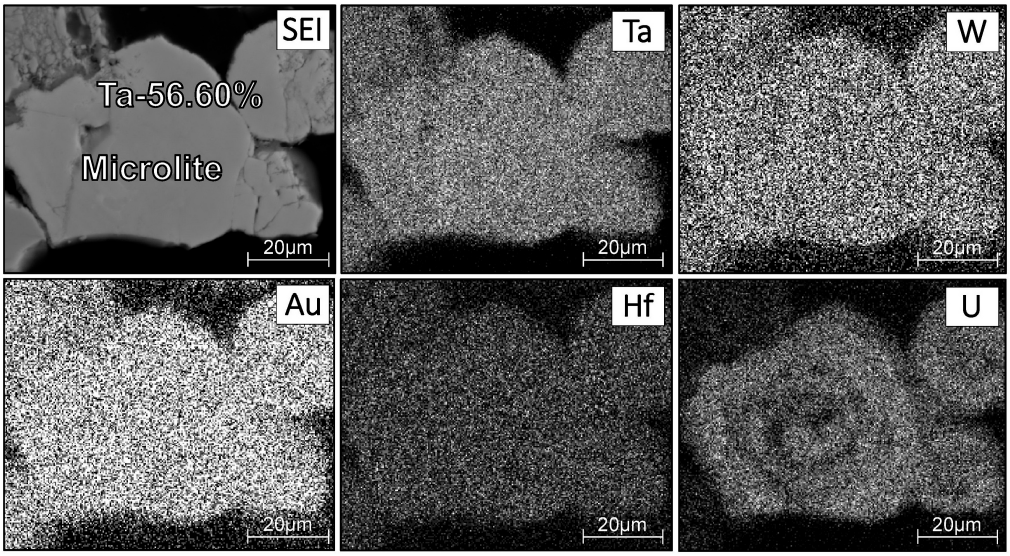

Figure 16. SEM images of microlite with nanometer Au, U, and W inclusions in pegmatite, Yubileinoye deposit.

Ixiolite, a typical base metal phase, is a Sn-bearing variety of tantalite occurring as pyramidal crystals with dihedral and pinacoidal faces (Figure 17a). According to its reflectance in polished sections, the mineral is close to weakly anisotropic tantalite and has relatively high contents of Sn (>1 wt.%) and Mn (0.9 wt.%). According to SEM data, ixiolite enclosed in cassiterite contains 38.9 wt.% Ta, 30.36 wt.% Sn, 5.01 wt.% Mn, 0.96 wt.% Fe, and 1.17–1.33 wt.% Au (Figure 17b). Ixiolite-greisen assemblages also bear native gold. Generally, rare-metal pegmatites of the area store some gold, but the issue requires further investigation.

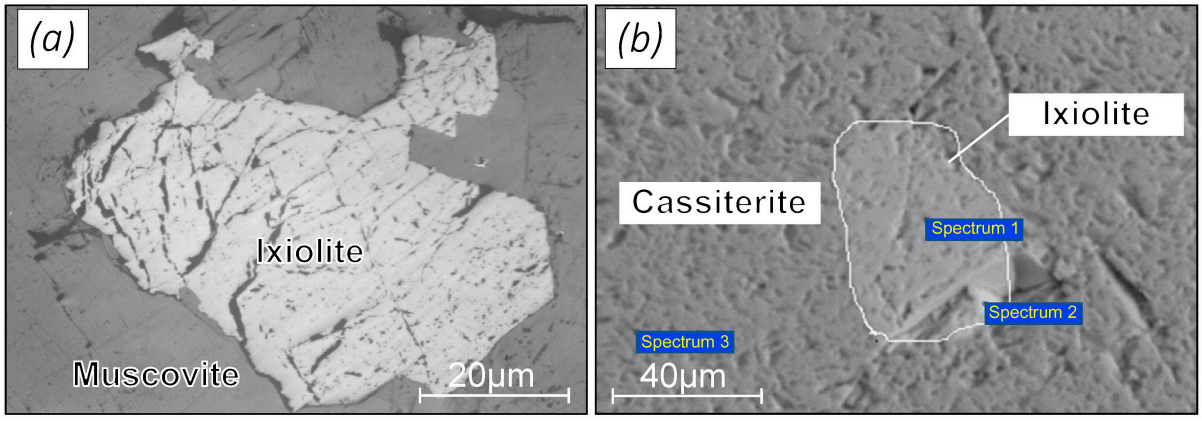

Figure 17. Ixiolite in a greisen assemblage from Yubileinoye deposit: ixiolite in muscovite (**a**); ixiolite in monomineralic cassiterite (**b**).

Table 1. ICP-MS analyses of trace elements (ppm) in Ta-bearing phases.

Sample	Deposit	Ta	Nb	Be	Li	Rb	Cs	Sn	W	Mo	Ta/Nb	ΣLi+Rb+Cs
K-12	Yubileinoye	199,160	271,100	4.43	117.1	17.4	2.9	972.2	122.2	0.59	0.73	137.4
50	Yubileinoye	349,700	125,810	0.76	276.6	78.29	48.91	53,890	2144	0.84	2.78	403.8
137	Yubileinoye	165,200	89,700	0.2	157.1	82.41	30.5	1840	168.9	1.28	1.84	270.01
2212-4	Yubileinoye	221,100	38,880	1.76	340.9	223.7	47.25	100,230	240.9	1.77	5.69	611.85
8077	Yubileinoye	35,300	5960	320.7	12,950	368.2	217.7	5250	18.83	4.78	5.92	13,536
Zh-100-a	Bakennoye	217,600	242,000	0.58	225.6	10	1.04	1092	72.8	1.37	0.9	236.64
11-D-a	Kvartsevoye	177,970	112,300	33.12	225.1	1174	162.3	2253	213.4	1.28	1.58	1561.4
9-a	Medvedka	98,560	152,100	26.52	19.22	42.03	5.69	752.1	2218	1.25	0.65	66.94
4071-a	Medvedka	24,210	67,310	1.2	11.87	16.88	2.54	683.4	339.2	0.67	0.36	31.29
4125	Urunkhay	87,370	182,100	31.8	76.72	63.43	5.63	669.5	736.7	1.65	0.48	145.78
20	Chinese Altai	40,110	44,150	6.2	97.8	19.2	25	118.7	21.33	4.25	0.91	142

Most of lithium in the Kalba-Narym zone resides in spodumene, lepidolite, muscovite, and pollucite from spodumene pegmatites composed of albite-spodumene, quartz-spodumene, and spodumene-cleavelandite-lepidolite assemblages.

Spodumene of pyroxene group (Li, Al [Si_2O_6]) exists as thick platy yellowish-white or beige prismatic crystals (some reaching 50 cm) with vitreous luster, which become pinkish upon alteration. Some spodumene crystals have preferred orientations and coexist with quartz, cleavelandite, and amblygonite (Figure 18). Main faces in prismatic spodumene are m {110} and pinacoidal a {100}. Spodumene contains mainly light rare earths, relatively high concentrations of Cu (107.30 ppm), Zn (116.40 ppm), and Pb (410.60 ppm), as well as 40.30 ppm Sb, 17.52 ppm Ag, 0.22 ppm Au, trace-element contents of 83.88 ppm Ga, 19.59 ppm Ge, 70.03 ppm Tl, and 72.13 B, and siderophile elements of Fe (11,500 ppm), Ni (118 ppm), and Cr (117 ppm). Major elements are Al (171,330 ppm), Ca (14,600 ppm), Mg (3531 ppm), and Na (10,722 ppm). The Li and Sn concentrations reach, respectively, 55,260 ppm and 217.4 ppm (Table 2). The Li contents are comparable to those in spodumene (5–6% Li_2O) from deposits of Zimbabwe, Greenbushes, etc. [31,32].

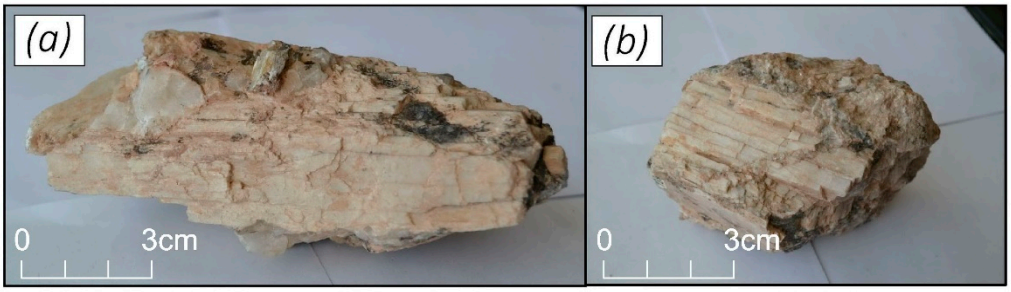

Figure 18. Typical spodumene, quartz-cleavelandite-spodumene assemblage: prismatic crystal (**a**); nest-like aggregates (**b**).

Table 2. ICP-MS analyses of trace elements (ppm) in spodumene.

Sample	Deposit	Ta	Nb	Be	Li	Rb	Cs	Sn	W	Mo
Zh-100-b (1)	Bakennoye	11.27	7.32	1.49	55,260	10.81	5.24	217.4	17.5	1.27
Zh-100-b (2)	Bakennoye	60.90	62.40	1.49	14,610	26.60	7.14	146.9	0.90	1.22
O-25	Bakennoye	0.30	2.64	1.17	48,130	114.0	15.54	69.29	7.59	1.30
M-4	Bakennoye	2.67	8.57	2.00	34,500	74.70	54.70	210.0	0.23	1.12
SP	Koktogai	84.15	41.76	102.0	53,040	24.07	33.13	3.85	1.30	38.21
B-1	Bakennoye	1.2	4.6	44.1	31,150	17.7	18.1	91.41	0.79	23.45
Yu-1	Bakennoye	3.6	13.7	1.06	20,070	12.4	256.8	59.63	0.94	4.17

SEM images (Figure 19a,b) reveal round inclusions of cassiterite in spodumene (37.95 wt.% Sn, 46.63 wt.% O), and >10 μm grains of a previously undetected iron silicate phase corresponding to $FeSiO_3$ ferrosilite. It occurs as irregularly shaped flaky inclusions (Figure 19c,d) and contains 65.22 wt.% Fe, 10.84 wt.% Si, 16.34 wt.% O, and impurities of Al (6.46 wt.%), Cr (0.58 wt.%), and Mn (0.56 wt.%). Minor amounts of ferrosilite are present in muscovite from the Bakennoye deposit and in beryl from pegmatite occurrences in Karkaraala. Microinclusions of iron silicates appear as clusters or grains (tens to hundreds of μm) in quartz-vein Sn, W deposits of the Kalba-Narym zone. Some grains contain 55.25 wt.% Fe, 8.55 wt.% Si, and 36.19 wt.% O (Figure 19e). Other varieties bear Al (6.05 wt.%), K (3.69 wt.%), and Na (1.43 wt.%) impurities (Figure 19f).

Late mineral assemblages include REE phases, such as monazite (with 2.33 wt.% Ag), Ir-bearing xenotime, and an F-bearing phase, presumably lessingite (Figure 20).

U-bearing xenotime is a typical phase of potentially Li-bearing albitized granites, like the Alakha (Gorny Altai) or New Akhmirovo deposits [33]. It often coexists with zircon, columbite, apatite, cassiterite, and fluorite. The trace-element composition is 32.86 wt.% Y,

14.13 wt.% P, 33.57 wt.% O, 4.95 wt.% Dy, 4.13 wt.% U, 3.31 wt.% Yb, 2.64 wt.% Er, 2.00 wt% Gd, etc.

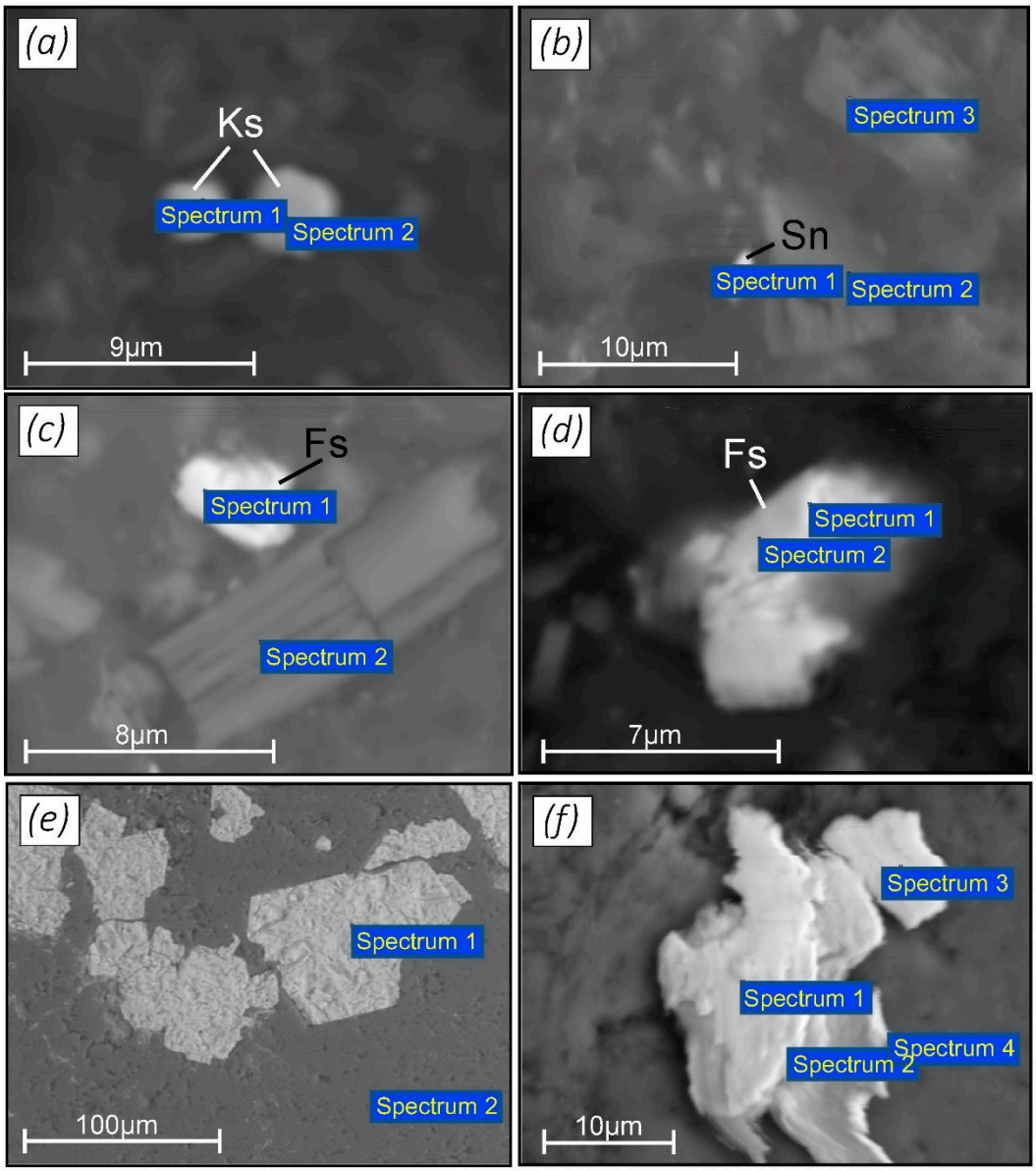

Figure 19. Microinclusions in spodumene and rare-metal pegmatite: cassiterite (**a**); native tin (**b**); flaky (**c**) and fuzzy (**d**) ferrosilite in spodumene, Bakennoye deposit; ferrosilite nests in rare-metal pegmatite (**e**,**f**).

Lepidolite is a main Li mineral in the quartz-cleavelandite-lepidolite (greisen) assemblage and one of principal indicators of rare-metal mineralization. It can occur either as coarse and medium flaky particles coexisting with large aggregates of cleavelandite and quartz, or as fine to very fine flaky metasomatic quartz-lepidolite nests among other minerals. It contains anomalously high concentrations of rare alkalis (16,240 ppm Li, 10,300 ppm Rb, and 1350 ppm Cs), relatively high contents of many trace elements (7470 ppm Ta, 109.5 ppm Nb, 81.5 ppm Sn, and 70.4 ppm W), and some trace elements above the average upper continental crust values [24] (1101 ppm B, 15.9 ppm Ge, 9.7 ppm Tl, 3001 ppm Mn, and 1372 ppm P). Lepidolite sheets enclose micrometer grains of metasomatic quartz which, in its turn, contains randomly distributed pollucite inclusions.

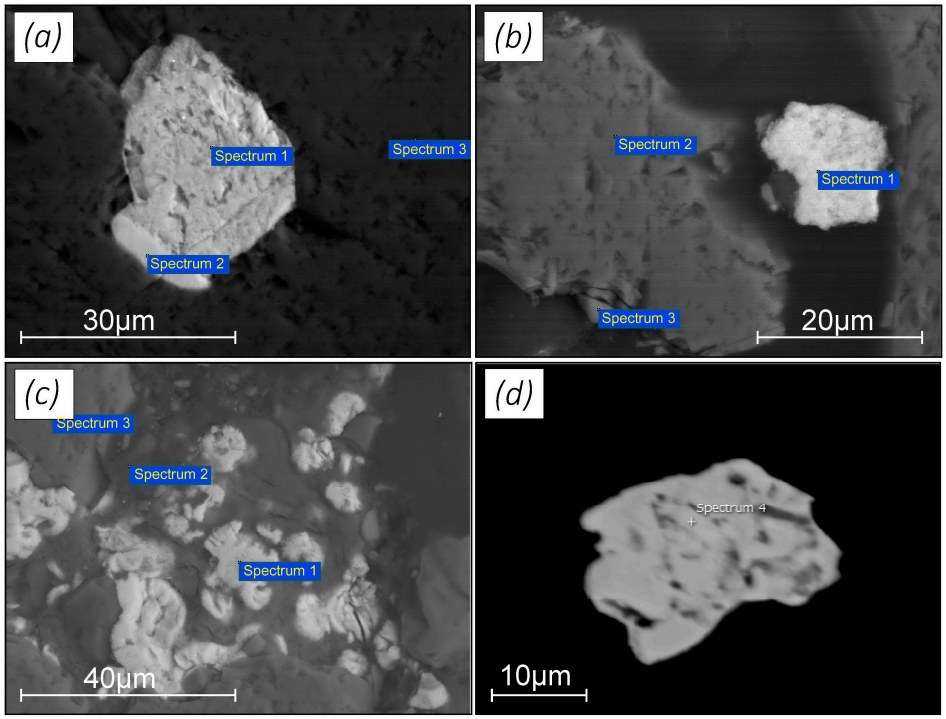

Figure 20. Microinclusions of REE phases: monazite (**a**); flakes (**b**) and nests (**c**) of F-bearing lessingite (?); U-bearing xenotime in albitized granite (**d**).

Transparent muscovite (and its greenish or gilbertite varieties) from different assemblages are main hosts of rare metals and rare alkalis. The total of rare alkalis reaches 12,308 ppm, and the contents of metals determined by ICP-MS are 153.1 ppm Ta, 301.1 ppm Nb, 35.9 ppm Be, 509.5 ppm Sn, and 25.9 ppm W. The crystals bear fluid inclusions (tantalite-columbite, cassiterite, fluorite, ilmenite, tetrahedrite, zircon, pyrite, barite, halite) and metallic species of Fe, Pb, etc.; some samples contain Ga (165 ppm) and Ag (11.8 ppm). The trace element contents in mica minerals increase as the mineralization progresses.

Color tourmalines are diverse in color, crystal morphology, and chemistry. Black tourmaline (shorl) with low trace-element abundances corresponds to simple pegmatite. The color varieties include aggregates of dark green tourmalines of variable coloration, blue indigolite, pink rubellite, and black-head polychrome tourmaline. Paragenetic assemblages of color tourmaline with cleavelandite, lepidolite, and pollucite are indicators of rich Ta, Nb, Sn, Li, and Cs ores; polychrome tourmaline with high Cs contents (1354 ppm) traces Cs ores.

Miarolitic pegmatite formed late during mineralization and is of limited occurrence. It is a gemstone facies widespread in Siberia, Tajikistan, Mongolia, and USA. In Eastern Kazakhstan, miarole assemblages (topaz, morion, aguemarine, emerald) are known from the Delbegetei granitic intrusion, and crystal-bearing pegmatite occurs in the Akzhailau and Dungaly intrusions. The Yubileinoye miarolitic pegmatite mainly includes albite, microcline, quartz, muscovite, lepidolite, and apatite, and less often contains spodumene and fluorite. The typical assemblage in ores is tantalite-microlite-samarskite-fergusonite minerals, which is of minor economic value though.

5. Discussion

Mineral resources of base, noble, and rare metals in Eastern Kazakhstan are critical for sustainable development of the mining and metallurgical industry. Many complex ore, gold, and rare-metal deposits in the Great Altai province still retain high mineral potential [1,3]. Mineral exploration progress requires further research with advanced

technologies and methods [4], including mineralogical and geochemical studies of minerals as tracers of ore formation conditions.

The new data we have obtained on compositions of weathered ironstones [17] show that they bear free gold of fine dust to fine size fractions, with Ag, Cu, W, and Pt impurities, which is amenable to gravity and flotation concentration. According to mass spectrometry, the ironstones contain heavy rare earths, PGE, Cr, Ni, Sr, and U. The typical main (goethite, limonite, magnetite, arsenopyrite, antimonite, and gold) and accessory (galena, chalcopyrite, sphalerite, brownite, cassiterite, etc.) phases and trace elements, such as Fe, Mn, As, Sb, Pb, Sn, Ag, and Au, can be used as exploration guides for deposits of this kind. The mineralogical exploration methods are especially useful in the case of hidden (buried) ores at initial prospecting stages [1].

The discussion on a large age range of primary gold mineralization at the Suzdal deposit [19] appears unreasonable as the gold-bearing structures were proven to be truncated by the Early Permian granites of the Kalba complex and volcanics of the Semeytau trough [34].

The Kalba-Narym rare-metal pegmatite deposits are traceable by an assemblage of unique minerals discovered at the macro- and microscopic levels (albite, cleavelandite, lepidolite, color tourmaline, spodumene, ambligonite, pollucite, tantalite-columbite, etc.) [9,10]. These minerals are common to large pegmatite fields worldwide (Bernic Lake, Zimbabwe, Vauchi, Zhiraul, Angola, Koktogai, etc.), but the Kalba mineralization differs in formation conditions and extent. The Kalba small pegmatite deposits occur in compositionally similar Late Devonian schists of the Takyr Fm., whereas the other deposits are found in older more mafic rocks (amphibolite, altered gabbro, etc.) [31,32].

The deposits of Eastern Kazakhstan formed in an alkaline granite-pegmatite system. The system gained trace elements (Ta, Nb, Be, Li, and Cs) mainly late during the process, as it is common for many such deposits [35]. The richest pegmatite veins show multistage mineralization and store diverse assemblages. The compositions of Ta minerals evolved from columbite to tantalite-columbite, manganotantalite, ixiolite, and microlite, judging by the corresponding increase in Mn/Fe and Ta/Nb ratios. Tantalite is enriched in rare alkalis, Sn, W, and contains Au, Ag, Pt, Ir, and In. Microlite contains relatively high Zr, Hf, and U, in the same way as that from the Giraúl field in Angola where late-generation tantalite is rich in Ta, Mn, Zr, and other elements [35].

Rare-metal mineralization can be predicted proceeding from the presence of spodumene, muscovite, and lepidolite, which are likewise common to pegmatites and rare-metal granites [9,36]. Li-bearing mica phases are important sources of lithium. In view of the growing demand for lithium in the world markets, it is pertinent to estimate pegmatite sites for the Sn-Be-Ta-Li potential.

Thus, the reported studies of gold and rare-metal mineralization provide new evidence for the composition of metal-laden fluids and the patterns of rare metals, REE, Au, and other elements that can be used as tracers of magmatism-related mineralization. The revealed mineral assemblages record the evolution of fluid regime and multistage ore formation, as one can infer by analogy with published evidence [18,29,32,37,38].

6. Conclusions

The studies of gold and rare-metal mineralization in Eastern Kazakhstan shed new light on the contents of rare metals, REE, Au, PGE, and other related elements in rare-metal phases. The analyzed samples from the Kalba deposits contain disseminated and free gold with Ag, Cu, and Pt impurities, and newly discovered rare mineral phases (alamosite, kentrolite, bunsenite, microlite, ferrosilite, etc.). Gold-bearing sulfides are traced by such elements as Fe, Mn, As, Sb, Cu, Pb, Zn, Ag, Sn, W, and Ba. A number of unique minerals (cleavelandite, lepidolite, color tourmalines, spodumene, ambligonite, pollucite, and tantalite-columbite), which are commonly found in other such deposits worldwide (Bernic Lake, Zimbabwe, Koktogai, etc.), are guides to rare-metal mineralization. The concentrations of Sn-Ta and Li-Cs increased progressively at the late stage of the pegmatitic

process. The analyses reveal diverse Ta-bearing minerals with Au, Ag, Pt, Zr, Hf, W, U, and Ir impurities that remained mute for semi-quantitative spectral analyses. Mica minerals (muscovite, lepidolite) are rich in Li and, together with spodumene, can be a source of lithium. The results have expanded the knowledge on the composition of ores and rocks, as well as on gold and rare metal mineralization patterns, which can have theoretical and practical applications in mineral exploration.

Author Contributions: B.A.D., A.Y.B. and M.A.M. elaborated the subject and main idea of the paper; methodology M.A.M. and N.A.Z.; software A.Y.B., T.A.O. and S.S.A.; validation B.A.D., A.Y.B. and S.V.K.; investigation B.A.D., M.A.M., T.A.O., A.Y.B. and N.A.Z.; resources B.A.D., O.N.K. and T.A.O.; data curation M.A.M. and O.N.K.; writing—original draft preparation B.A.D. and A.Y.B.; writing—review and editing B.A.D., A.Y.B., S.V.K. and M.A.M.; visualization M.A.M. and S.V.K.; supervision S.V.K.; project administration B.A.D.; funding acquisition B.A.D. All authors have read and agreed to the published version of the manuscript.

Funding: The research was additionally funded by the Science Committee of the Ministry of Education and Science of the Republic of Kazakhstan (Grant No. AP08856325). The research was carried out on a government assignment to the V.S. Sobolev Institute of Geology and Mineralogy (Novosibirsk).

Data Availability Statement: The data presented in this study are available on request from the corresponding author.

Acknowledgments: We wish to thank our colleagues E. Sapargaliev for assistance in the field, as well as A. Vladimirov, I. Annikova, and M. Kuibida for advice and discussions. Thanks are extended to analysts A. Rusakova, S. Polezhaev, and A. Sadibekov for laboratory work. Thanks are extended to Tatiana Perepelova for aid in manuscript preparation.

Conflicts of Interest: The authors declare no conflict of interest.

References

1. *The Great Altai—Unique Rare Metal-Gold-Polymetallic Province of Central Asia*; Prof. Conference: Almaty, Kazakhstan, 2019; 60p. (In Russian)
2. Dyachkov, B.; Mizernaya, M.; Kuzmina, O.; Zimanovskaya, N.; Oitseva, T. Tectonics and metallogeny of East Kazakhstan. In *Tectonics. Problems of Regional Setting*; IntechOpen Limited: London, UK, 2018; pp. 67–84. [CrossRef]
3. Shcherba, G.N.; Bespayev, K.H.; D'yachkov, B.; Mysnik, A.; Ganzhenko, G.; Sapargaliyev, E. *Great Altai: Geology and Metallogeny. Book 2. Metallogeny*; RIO VAK RK: Almaty, Kazakhstan, 2000; 400p. (In Russian)
4. D'yachkov, B.A.; Omirserikov, M.S.; Sapargaliyev, E.M.; Oitseva, T.A.; Kuzmina, O.N.; Zimanovskaya, N.A. Improving mineral exploration technologies: Theoretical background. In *Innovations and Progressive Exploration Technologies in Kazakhstan*; Proc. Conference: Almaty, Kazakhstan, 2017; pp. 21–25. (In Russian)
5. D'yachkov, B.A.; Titov, D.V.; Sapargaliev, E.M. Ore belts of the Greater Altai and their ore resource potential. *Geol. Ore Deposit.* **2009**, *51*, 197–211. [CrossRef]
6. Chekalin, V.M.; D'yachkov, B.A. Rudny Altai base-metal belt: Localization of massive sulfide mineralization. *Geol. Ore Deposit.* **2013**, *55*, 438–454. [CrossRef]
7. Mizernaya, M.; Aitbayeva, S.; Mizerny, A.; D'yachkov, B. Geochemical characteristics and metallogeny of Herzinian granitoid complexes (Eastern Kazakhstan). Natsionalnyi Hirnychyi Universytet. *Naukovyi Visnyk* **2020**, *1*, 5–10. [CrossRef]
8. Kuz'mina, O.; D'yachkov, B.; Vladimirov, A.; Kirillov, M.; Redin, Y.O. Geology and mineralogy of East Kazakhstan gold-bearing jasperoids (by the example of the Baybura ore field). *Russ. Geol. Geophys.* **2013**, *54*, 1471–1483. [CrossRef]
9. Oitseva, T.A.; D'yachkov, B.A.; Vladimirov, A.G.; Kuzmina, O.N.; Ageeva, O.V. New data on the substantial composition of Kalba rare metal deposits. *Iop C Ser. Earth Environ.* **2017**, *110*, 0120183. [CrossRef]
10. Khromykh, S.V.; Oitseva, T.A.; Kotler, P.D.; D'yachkov, B.A.; Smirnov, S.Z.; Travin, A.V.; Vladimirov, A.G.; Sokolova, E.N.; Kuzmina, O.N.; Mizernaya, M.A.; et al. Rare-metal pegmatite deposits of the Kalba Region, Eastern Kazakhstan: Age, composition and petrogenetic implications. *Minerals* **2020**, *10*, 1017. [CrossRef]
11. Zonenshain, L.P.; Kuzmin, M.I.; Natapov, L.M. *Geology of the USSR: A Plate Tectonic Synthesis. Geodynamic Series 21*; American Geophysical Union: Washington, DC, USA, 1990; 242p.
12. Filippova, I.B.; Bush, V.A.; Didenko, A.N. Middle Paleozoic subduction belts: The leading factor in the formation of the Central Asian fold-and-thrust belt. *Russ. J. Earth Sci.* **2001**, *3*, 405–426. [CrossRef]
13. Vladimirov, A.G.; Kruk, N.N.; Rudnev, S.N.; Khromykh, S.V. Geodynamics and granitoid magmatism of collision orogens. *Russ. Geol. Geophys.* **2003**, *44*, 1321–1338.
14. Windley, B.F.; Alexeiev, D.; Xiao, W.; Kröner, A.; Badarch, G. Tectonic models for accretion of the Central Asian Orogenic Belt. *J. Geol. Soc.* **2007**, *164*, 31–47. [CrossRef]

15. Vladimirov, A.G.; Kruk, N.N.; Khromykh, S.V.; Polyansky, O.P.; Chervov, V.V.; Vladimirov, V.G.; Travin, A.V.; Babin, G.A.; Kuibida, M.L.; Khomyakov, V.D. Permian magmatism and lithospheric deformation in the Altai caused by crustal and mantle thermal processes. *Russ. Geol. Geophys.* **2008**, *49*, 468–479. [CrossRef]
16. Barannikov, A.G.; Ugryumov, A.N. Problems of endogenous gold oreforming of Urals Mesozoic. *Lithosphere.* **2003**, *1*, 13–26.
17. Rafailovich, M.; Mizernaya, M.; D'yachkov, B. *Large Gold Deposits in Black Shales: Formation Conditions and Features of Similarity*; Luxe Media Group: Almaty, Kazakhstan, 2011; 272p. (In Russian)
18. Naumov, E.A.; Borovikov, A.A.; Borisenko, A.S.; Zadorozhniy, M.V.; Murzin, V.V. Physicochemical conditions of formation of epithermal gold-mercury deposits. *Russ. Geol. Geophys.* **2002**, *43*, 1003–1013.
19. Kovalev, K.; Kalinin, Y.A.; Naumov, E.; Pirajno, F.; Borisenko, A. A mineralogical study of the Suzdal sediment-hosted gold deposit, Eastern Kazakhstan: Implications for ore genesis. *Ore Geol. Rev.* **2009**, *35*, 186–205. [CrossRef]
20. Kovalev, K.; Kuzmina, O.; Dyachkov, B.; Vladimirov, A.; Kalinin, Y.A.; Naumov, E.; Kirillov, M.; Annikova, I.Y. Disseminated gold–sulfide mineralization at the Zhaima deposit, eastern Kazakhstan. *Geol. Ore Deposit.* **2016**, *58*, 116–133. [CrossRef]
21. Khromykh, S.V.; Tsygankov, A.A.; Kotler, P.D.; Navozov, O.V.; Kruk, N.N.; Vladimirov, A.G.; Travin, A.V.; Yudin, D.S.; Burmakina, G.N.; Khubanov, V.B.; et al. Late Paleozoic granitoid magmatism of Eastern Kazakhstan and Western Transbaikalia: Plume model test. *Russ. Geol. Geophys.* **2016**, *57*, 773–789. [CrossRef]
22. Khromykh, S.V.; Kotler, P.D.; Izokh, A.E.; Kruk, N.N. A review of Early Permian (300–270 Ma) magmatism in Eastern Kazakhstan and implications for plate tectonics and plume interplay. *Geodyn. Tectonophys.* **2019**, *10*, 79–99. [CrossRef]
23. D'yachkov, B.A.; Mataibaeva, I.E.; Frolova, O.V.; Gavrilenko, O.D. Types of rare metal deposits in East Kazakhstan and mineral potential estimation. *Gornyi Zhurnal* **2017**, *#8*, 45–50. [CrossRef]
24. Rudnick, R.L.; Gao, S. Composition of the Continental Crust. In *Treatise on Geochemistry*; Holland, H.D., Turekian, K.K., Eds.; Elsevier Science: Amsterdam, The Netherlands, 2003; Volume 3, pp. 1–64. [CrossRef]
25. Palache, C.; Merwin, H. Alamosite, a new Lead Silicate from Mexico. *Amer. J. Sci.* **1909**, *27*, 399–401. [CrossRef]
26. Perova, E.N. Rare minerals of manganese ores from the Zhomart deposit. In *Metallogeny of Kazakhstan*; Proc. Conference: Almaty, Kazakhstan, 2017; pp. 124–126. (In Russian)
27. Britvin, S.; Kolomensky, V.; Boldyreva, M.; Bogdanovs, A.; Kretser, Y.; Boldyreva, O.; Rudashevsky, N. Nickelphosphide (Ni, Fe)3P, a nickel analog of Schreibersite. *Zapiski VMO* **1999**, *128*, 64–72.
28. O'Driscoll, B.; Clay, P.L.; Cawthorn, R.G.; Lenaz, D.; Adetunji, J.; Kronz, A. Trevorite: Ni-rich spinel formed by metasomatism and desulfurization processes at Bon Accord, South Africa. *Mineralog. Magaz.* **2014**, *78*, 145–163. [CrossRef]
29. Zagorsky, V.Y.; Vladimirov, A.; Makagon, V.; Kuznetsova, L.; Smirnov, S.; D'yachkov, B.; Annikova, I.Y.; Shokalsky, S.; Uvarov, A. Large fields of spodumene pegmatites in the settings of rifting and postcollisional shear–pull-apart dislocations of continental lithosphere. *Russ. Geol. Geophys.* **2014**, *55*, 237–251. [CrossRef]
30. Tang, Y.; Wang, H.; Zhang, H.; Lv, Z.-H. K-feldspar composition as an exploration tool for pegmatite-type rare metal deposits in Altay, NW China. *J. Geochem. Explor.* **2018**, *185*, 130–138. [CrossRef]
31. Tkachev, A.V.; Rundqvist, D.V.; Vishnevskaya, N.A. Metallogeny of lithium through geological time. *Russ. J. Earth Sci.* **2018**, *18*, 1–13. [CrossRef]
32. Dittrich, T.; Seifert, T.; Schulz, B.; Hagemann, S.; Gerdes, A.; Pfänder, J. *Archean Rare-Metal Pegmatites in Zimbabwe and Western Australia. Springer Briefs in World Mineral Deposits*; Springer: Cham, Switzerland, 2019; 125p. [CrossRef]
33. Annikova, I.Y.; Vladimirov, A.G.; Smirnov, S.Z.; Oitseva, T.A.; Mikheev, E.I.; Jes, E.N.; Travin, A.V.; D'yachkov, B.A.; Maslov, V.I.; Gertner, I.F. Geology and mineralogy of the Novo-Akhmirovskoe deposit of lithium topaz-zinnwaldite granites (East Kazakhstan). *Lithosphere* **2019**, *19*, 304–326. [CrossRef]
34. D'yachkov, B.; Kuzmina, O.; Zimanovskaya, N.; Mizernaya, M.; Chernenko, Z.; Amralinova, B. *Types of Gold Deposits in Eastern Kazakhstan*; EKSTU: Ust-Kamenogorsk, Kamenogorsk, 2015; 150p. (In Russian)
35. Gonçalves, A.O.; Melgarejo, J.-C.; Alfonso, P.; Amores, S.; Paniagua, A.; Neto, A.B.; Morais, E.A.; Camprubí, A. The distribution of rare metals in the LCT pegmatites from the Giraúl Field, Angola. *Minerals* **2019**, *9*, 580. [CrossRef]
36. D'yachkov, B.; Aitbayeva, S.; Mizernaya, M.; Amralinova, B.; Bissatova, A. New data on non-conventional types of East Kazakhstan rare metal ore. *Sci. Bull. Nat. Min. Univ.* **2020**, 11–16. [CrossRef]
37. Dyachkov, B.; Mizernaya, M.; Zhunusov, A.; Miroshnikova, A.; Aitbayeva, S.; Umarbekova, Z.; Bissatova, A. Formation features and prediction criteria for gold-sulphide deposits (East Kazakhstan). *Inter. J. Adv. Tren. Comp. Sci. Eng.* **2020**, *9*, 8758–8762. [CrossRef]
38. Zimanovskaya, N.; Gavrilenko, O. Gold in massive sulfide (base metal) and carbonaceous gold sulfide deposits in Eastern Kazakhstan. *Eurasian Min.* **2014**, *1*, 49–53.